Research Article

Muhammad Farooq, Rashid Nawaz, Alamgeer Khan, Bakri Adam Younis, Fathi Mohammed DawAlbait, and Gamal M. Ismail*

Comparative study of couple stress fluid flow using OHAM and NIM

https://doi.org/10.1515/phys-2024-0038
received December 23, 2023; accepted May 07, 2024

Abstract: In this article, the plane Poiseuille flow of couple stress fluid of Vogel's model between two parallel plates under the influence of non-isothermal effects have been investigated using Optimal homotopy asymptotic method (OHAM) and New iterative method (NIM). The governing continuity and momentum equations are transformed to ordinary differential equations and the coupled system of differential equations is then explored using the said methods. The expressions for velocity profile, temperature distribution, average velocity, volume flux, and shear stress have been obtained employing the said methods. Various essential flow properties have been presented and discussed. The results acquired *via* these techniques are in the form of infinite series; thus, the results can be effortlessly calculated. Comparison of both techniques are illustrated with the help of different tables and graphs and found both methods to be in a good agreement. Consequently, it will be more appealing for the investigators to apply the proposed methods to diverse problems arising in fluid dynamics.

Keywords: plane Poiseuille flow, non-isothermal effects, coupled system of differential equations.

Nomenclature

A_1	first Rivlin-Ericksen tensor
c_p	specific heat (J/kg K)
$\frac{D}{Dt}$	material derivative
H	dimensional temperature (K)
H_0	lower plate temperature (K)
H_1	upper plate temperature (K)
H^*	dimensionless temperature
I	unit tensor
J	body force
κ	thermal conductivity (W/m K)
p	dynamic pressure (N/m^2)
z	first component of dimensional velocity
z^*	first component of dimensionless velocity
ϕ	velocity vector (m/s)
μ	dimensional coefficient of viscosity
ρ	constant density (kg/m^3)
Ω	gradient of ϕ
μ_0	reference viscosity
μ^*	dimensionless coefficient of viscosity
τ	Cauchy stress tensor
η	couple stress parameter

1 Introduction

Recently, the non-Newtonian fluids have more attention than Newtonian fluids for scientists and researchers, due to its wide range applications in industries and technology [1,2]. It has countless practical applications in modern industries and technology, and headed many scientists to attempt diverse non-Newtonian fluid flows problems. One such fluid that has attracted scientists and researchers in fluid mechanics during the last few decades is the couple stress fluids theory proposed by Stokes [3]. Because of the complexity of the non-Newtonian fluids, it cannot be fitted into a single constitutive model, so various constitutive models for different categories of the said fluids have been proposed. The notion of couple stresses fluids arise

* **Corresponding author: Gamal M. Ismail**, Department of Mathematics, Faculty of Science, Islamic University of Madinah, 42351, Madinah, Saudi Arabia, e-mail: gismail@iu.edu.sa
Muhammad Farooq, Alamgeer Khan: Department of Mathematics, Abdul Wali Khan University, Garden Campus, Mardan, KP, Pakistan
Rashid Nawaz: UniSA STEM, University of South Australia, Adelaide, Australia
Bakri Adam Younis: Department of Mathematics, College of Arts and Science in Elmgarda, King Khalid University, Abha, Saudi Arabia
Fathi Mohammed DawAlbait: Department of Science and Technology, Ranyah University College, Taif University, Ta'if, Saudi Arabia

due to the approach of how the mechanical interactions of the fluid medium can be modeled. The said theory well depicts the flow behavior of fluids taking a substructure, *e.g.*, lubricants with polymer additives, animal blood, and liquid crystals [3,4].

Among the numerous models, that are used to explain the non-Newtonian behavior, presented by certain fluids, the couple stresses fluids attained surprising attention [5,6]. The couple stress fluids model characterizes those fluids which contain randomly oriented and rigid particles suspended in a viscous medium. The stress tensor in those fluids is anti-symmetric; therefore, the exact behavior of flows cannot be predicted in classical Newtonian theory. The significant characteristic of this model is that, the solutions of differential equations are like that of Navier–Stokes equations. This model has been used frequently, because of its mathematical simplicity, as compared to other established fluid models under consideration. The couple stress fluid theory has applications in lubricants with animal blood, polymer additives, and liquid crystals. Many research works have been performed on the hydrodynamic lubrication of squeezing film flows, treating the lubricant as a couple stress fluid. The studies demonstrated that the couple stress fluid enhances the load-carrying capacity of the journal bearing [7–9].

There is a rising industrial demand to develop the thermal properties of fluid as they flow over surfaces. Practical applications contain coolants in heat transfer [10,11], mass transfer [12], electronics [13], and heat exchangers [14,15]. The study of heat transfer flow is significant in numerous engineering applications, for instance, the design of thrust bearing, drag reduction, transpiration cooling, radial diffusers, and thermal recovery of oil. Heat transfer has a vital role in handling and processing of non-Newtonian mixtures [16,17].

Literature has investigated flow issues using a variety of methods. The primary approaches for determining approximations of flow issue solutions include numerical techniques, iterative techniques, perturbation methods, and homotopy-based techniques. Every method has its pros and cons. Discretization is employed in numerical approaches, which has an impact on accuracy. These techniques need a significant amount of time and processing. Strong nonlinear problems do not yield more accurate findings when utilizing numerical techniques. There are certain restrictions on perturbation approach as well, for instance the supposition of a small parameter and high nonlinearity.

One of the methods for solving differential equations based on power homotopy is the optimal homotopy asymptotic method (OHAM). In order to solve differential equations, Marinca *et al.* [18] first presented this method in 2008. Unlike other numerical techniques, it does not require discretization and, in contrast to other perturbation techniques, is applicable even in the dearth of tiny or large parameters. In contrast to iterative approaches [18,19], this method does not require an initial guess. Various issues have been addressed using this methodology [20,21]. The extremely nonlinear partial differential equations (PDEs) caused by the heat flux circumstances were converted by the authors in previous studies [22,23] into structure of ordinary differential equations (ODEs) with the appropriate conditions, and the OHAM evaluation method was then used to assess the results.

A novel method to solve linear and nonlinear equations, known as the new iterative method (NIM), was put out by Gejji and Jafari [24] in 2006. In the future, a large number of scientists and mathematicians may use NIM to solve a variety of problems, including those involving a system of nonlinear dynamical equations, ODE's, PDE's, algebraic equations, and evolution equations. In comparison to other analytical methods, this method yields results that rapidly converge [25,26]. The strongly nonlinear and coupled system of differential equations are investigated for shear stress, velocity, temperature distributions, average velocity, and volumetric flow rate on the plates using the two methods OHAM and NIM [27,28].

In the present study, the plane Poiseuille couple stress fluid flowing between two parallel walls maintained at various temperatures has been investigated. The temperature dependent viscosity is calculated using Vogel's model employing the OHAM and NIM. The coupled nonlinear ODEs have been explored using the aforementioned approaches, and various issues have been discussed.

This study contains six sections, Section 1 is for brief introduction, Section 2 is dedicated to basic governing equations and problem formulation, in Section 3, basic concepts of the methods are discussed, in Section 4, solution of the problem is given, Section 5 consists of results and discussions, and Section 6 gives the conclusion of the study.

2 Basic equations and problem formulation

2.1 Basic equations

The basic governing equations for balance of momentum, mass conservation, and energy of an incompressible fluid are given as follows [29,30]:

$$\nabla\cdot\phi = 0, \tag{1}$$

$$\rho\dot{\phi} = \nabla\cdot\ddot{\imath} - \eta\nabla^4\phi + \rho J, \tag{2}$$

$$\rho c_p\dot{\mathscr{H}} = \hat{h}\nabla^2\mathscr{H} + \ddot{\imath}\Omega, \tag{3}$$

where ϕ is the velocity, p is the constant density, $\hat{h}$ is the thermal conductivity, $\mathscr{H}$ is the temperature, J is the body force per unit mass, $\ddot{\imath}$ is the Cauchy stress tensor, the specific heat is denoted by c_p, also the gradient of ϕ is denoted by Ω, and here χ is used for couple stress parameter and the material derivative is represented by $\frac{D}{Dt}$ and is defined as follows:

$$\frac{D}{Dt}(*) = \left(\frac{\partial}{\partial t} + \phi.\ \nabla\right)(*), \tag{4}$$

$$\ddot{\imath} = -pI + \varpi A_1, \tag{5}$$

where p is the dynamic pressure, I is the unit tensor, ϖ is the coefficient of viscosity, and the first Rivlin-Ericksen tensor is represented by A_1 and is defined as

$$A_1 = \Omega + \Omega^t. \tag{6}$$

Here the transpose of Ω is denoted by Ω^t.

2.2 Problem formulation

Here we consider the plane Poiseuille flow of couple stress fluid of Vogel's between two parallel plates $2d$ apart, under the influence of non-isothermal effects, both walls are motionless as in Figure 1. The temperatures of lower and upper plates are $\mathscr{H}_0$ and $\mathscr{H}_1$, respectively. These walls are placed in the (x, y) axes orthogonal coordinate system in the plane at $y = d$, and $y = -d$, the motion of the fluid is in the x-axis direction and y-axis is perpendicular to the walls. The pressure gradient is zero, here velocity and temperature are

$$\phi = \phi(z, 0, 0), z = z(y), \text{and } \mathscr{H} = \mathscr{H}(y). \tag{7}$$

Eq. (1) is simultaneously fulfilled. In the absence of body force, Eqs. (2) and (3), *i.e.*, the momentum and energy equations become

$$\varpi(d^2z)/(dy^2) + (d\varpi)/dydz/dy - \chi(d^4z)/(dy^4) - A = 0, \tag{8}$$

$$\frac{d^2\mathscr{H}}{dy^2} + \left(\frac{\varpi}{\hat{h}}\right)((dz)/(dy))^2 - \left(\frac{\chi}{\hat{h}}\right)((d^2z)/(dy^2))^2 = 0. \tag{9}$$

The corresponding boundary conditions for Eqs. (8) and (9) are

$$z(-d) = 0, z(d) = \phi, \tag{10a}$$

$$z(-d)'' = 0, z(d)'' = 0, \tag{10b}$$

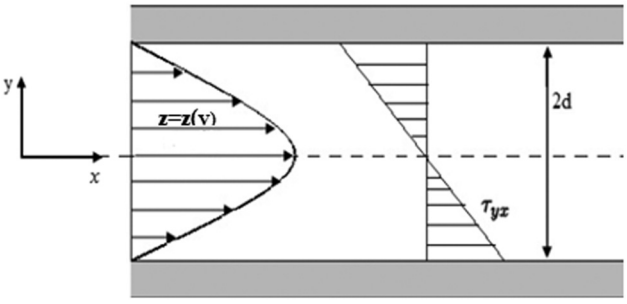

Figure 1: Geometry of plane Poiseuille flow.

$$\mathscr{H}(-d) = \mathscr{H}_0, \mathscr{H}(d) = \mathscr{H}_1. \tag{11}$$

The no-slip boundary conditions are Eq. (10a). Eq. (10b) indicates that the couple stress vanishes at the walls. For over-all use, the following dimensionless parameters are introduced:

$$z^* = \frac{z}{\phi}, \mathscr{H}^* = \frac{\mathscr{H} - \mathscr{H}_0}{\mathscr{H}_1 - \mathscr{H}_0}, \varpi^* = \frac{\varpi}{\varpi_0}, y^* = \frac{y}{d}, \beta = d\sqrt{\frac{\varpi_0}{\chi}},$$

$$\delta = \frac{\varpi_0\phi^2}{\hat{h}(\mathscr{H}_1 - \mathscr{H}_0)}.$$

Hence, by ignoring the asterisks, Eqs. (8) and (9) with boundary conditions (10a, 10b, and 11), become as under

$$\frac{d^4z}{dy^4} - \frac{\beta^2\varpi(d^2z)}{dy^2} - \frac{\beta^2(d\varpi)}{dy}\frac{dz}{dy} + A = 0, \tag{12}$$

$$\frac{d^2\mathscr{H}}{dy^2} + \delta\varpi\left(\frac{dz}{dy}\right)^2 + \frac{\delta}{\beta^2}\left(\frac{d^2z}{dy^2}\right)^2 = 0, \tag{13}$$

$$z(-1) = 0, z(1) = 1, z(-1)'' = 0, z(1)'' = 0, \tag{14}$$

$$\mathscr{H}(-1) = 0, \mathscr{H}(1) = 1. \tag{15}$$

The dimensionless Vogel's viscosity model [31,32] is as follows:

$$\varpi = \varpi_*\exp\left(\frac{A_0}{\beta_0 + \mathscr{H}} - \mathscr{H}_\varpi\right). \tag{16}$$

After using Taylor series expansion, we obtain

$$\varpi = \alpha^2\left(1 - \frac{A_0}{\beta_0 + \mathscr{H}}\right). \tag{17}$$

Here A_0, β_0, and $\alpha^2 = \exp\left(\frac{A_0}{\beta_0} - \mathscr{H}_\varpi\right)$ are viscosity parameters corresponding to Vogel's model. Assume that $A_0 = \varepsilon d$, where ε is a small parameter.

3 Description of the techniques

A concise introduction to OHAM and NIM are presented in this section.

3.1 Basic notion of OHAM

Consider the differential equation

$$L(z(x)) + J(x) + M(z(x)) = 0, \beta(z, \mathrm{d}z/\mathrm{d}x) = 0. \quad (18)$$

Here linear operator is denoted by L, J is the given function, z is the unknown function, to be determined, β is the boundary operator, and M is a nonlinear operator.

By OHAM [33]

$$(1 - m)[L(z(x, m)) + J(x))] = R(m)[L(z(x, m)) + J(x)) + M(z(x, m))],$$
$$\beta\left(z(x, m), \frac{\mathrm{d}z(x, m)}{\mathrm{d}x}\right) = 0, \quad (19)$$

here $m\varepsilon[0,1]$ is the embedding parameter, $R(m)$ is an auxiliary function such that for $m \neq 0$, $R(m) \neq 0$ and for $m = 0$, $r = 0$, *i.e.*, $R(0) = 0$, clearly when $m = 0$ and for $m = 1$ it gives

$$z(x, 0) = z_0(x), \quad z(x, 1) = z(x). \quad (20)$$

The solution $z(x, r)$ varies from $z_0(x)$, to the solution $z(x)$ as the embedding parameter, m varies from 0 to 1, we got $z_0(x)$, by using $m = 0$ in Eq. (18),

$$L(z_0(x)) + J(x) = 0, \beta\left(z_0\frac{\mathrm{d}z_0}{\mathrm{d}x}\right) = 0. \quad (21)$$

The auxiliary function $R(m)$ can be written as

$$R(m) = mc_1 + m^2c_2 + m^3c_3 + ..., \quad (22)$$

where $c_1 \ldots c_i$ are constants, the solution of Eq. (19) is as follows:

$$z(x, m, c_j) = z_0(x) + \sum_{i\geq 1} z_i(x, c_j)m^i, \quad j = 1, 2, ... \quad (23)$$

Substituting Eq. (23) in Eq. (19) and equating the like powers of m, we acquire the following system:

$$L(z_1(x)) = c_1M_0(z_0(x)), \beta\left(z_1\frac{\mathrm{d}z_1}{\mathrm{d}x}\right), \quad (24)$$

$$L(z_j(x) - z_{j-1}(x)) = c_jM_0(z_0(x)) + \sum_{k=1}^{j-1} c_k[L(z_{j-k}(x)) + M_{j-k}(z_0(x), z_1(x)\ldots z_{j-1}(x))]\beta\left(z_j\frac{\mathrm{d}z_j}{\mathrm{d}x}\right) j = 1, 2, \ldots \quad (25)$$

The term $M_r(z_0(x), z_1(x)\ldots z_r(x))$ in Eq. (25) is the coefficient of m^r in the expansion

$$M(z(x, m, c_k)) = M_0(z_0(x)) + \sum_{(j\geq 1)} M_j(z_0(x), z_1(x)\ldots z_j(x))m^j, \quad (26)$$
$$k = 1, 2, \ldots.$$

Eqs. (21), (24), and (25) can effortlessly be evaluated for $z_j(x)$, the solution of Eq. (23) is totally dependent on the constant c_k, if at $m = 1$, it is convergent, then Eq. (23) implies

$$z(x, c_j) = z_0(x) + \sum_{i\geq 1}^{l} z_i(x, c_j). \quad (27)$$

Generally, the solution of Eq. (18) is approximated as follows:

$$z^e(x, c_j) = z_0(x) + \sum_{i=1}^{l} z_i(x, c_j), \quad j = 1, 2, \ldots e. \quad (28)$$

After plugging Eq. (28) in Eq. (18), we gain the residual

$$R(x, c_j) = L(z^e(x, c_j)) + J(x) + M(z^e(x, c_j)), \quad j = 1, 2, \ldots e. \quad (29)$$

If the residual vanishes, *i.e.*, $R(x, c_j) = 0$ we achieve the exact solution $z^e(x, c_j)$, on the other hand, if $R(x, c_j) \neq 0$, we can minimize as follows:

$$J(c_j) = \int_a^b R^2(x, c_j)\mathrm{d}x, \quad (30)$$

where a and b are constants, depending on the chosen problem. $c_1, c_2, c_3 \ldots$ can be acquired using Eq. (30).

$$\frac{\partial J}{\partial c_i} = 0, \ i = 1, 2, ..., \quad r. \quad (31)$$

After we attained the values of unknown constants, $c_1, c_2, c_3 \ldots$, we can achieve the estimated solution using (28).

3.2 Basic notion of NIM

In this subsection, a brief introduction of NIM is given, assume the differential equation

$$z(x) = L(z(x)) + J(x) + M(z(x)). \quad (32)$$

Here linear operator is denoted by L, J is the given function, z is not known, to be determined, and M is a nonlinear operator. Assume that the NIM solution of Eq. (32) is in the form

$$z(x) = \sum_{i=0}^{\infty} z_i, \quad (33)$$

since L is linear, we have

$$L\left(\sum_{i=0}^{\infty} z_i\right) = \sum_{i=0}^{\infty} L(z_i). \tag{34}$$

The nonlinear operator is given as [24]

$$M\left(\sum_{i=0}^{\infty} z_i\right) = M(z_0(x)) + \sum_{i=1}^{\infty}\left\{M\left(\sum_{j=0}^{i}(z_j) - M\left(\sum_{j=0}^{i-1} z_j\right)\right\}\right. = \sum_{i=0}^{\infty}\phi(z_i), \tag{35}$$

where $\phi_0 = M(z_0(x))$ and

$$\phi_i = \left\{M\sum_{j=0}^{i}(z_j) - M\left(\sum_{j=0}^{i-1} z_j\right)\right\}. \tag{36}$$

Using Eqs. (33)–(35) in Eq. (32), we obtain

$$\sum_{i=0}^{\infty}(z_i) = J(x) + \sum_{j=0}^{i} L(z_j) + \sum_{i=0}^{\infty}\phi(z_i). \tag{37}$$

4 Solution of the problem

The solutions of velocity (z_o) and temperature $\mathscr{H}_0$ up to second order employing OHAM are

$$\begin{aligned} Z_o = {} & \frac{1}{24}(-0.4 + 0.48y^2 - 0.08y^4) + 0.0002755731922398589(0.03929001908488884 \\ & - 0.00000947015732976054 4y - 0.04830740051420759y^2 + 0.00001433321109369163 6y^3 \\ & + 0.009661480102841517y^4 - 0.00000537495416013436 3y^5 - 0.00064409867352276 79y^6 \\ & + 5.119003962032726 \times 10^{-7}y^7) + 5.900589299243685 \times 10^{-11}(-83.51967901698663 \\ & + 0.027130389292835844y + 103.20176810212433y^2 - 0.0420353390262278y^3 \\ & - 21.476017575703736y^4 + 0.017171546689390027y^5 + 1.8924118605914373y^6 \\ & - 0.002399201699659237y^7 - 0.10014490331166559y^8 + 0.000132603809649819 97y^9 \\ & + 0.001783061152899000 8y^{10} + 1.055893061153132 \times 10^{-9}y^{11} \\ & - 0.000121520900691187 79y^{12} - 1.279420141328451 \times 10^{-10}y^{13} \\ & - 6.994654768041515 \times 10^{-9}y^{14} + 6.053170561123858 \times 10^{-12}y^{15}) \end{aligned}, \tag{38}$$

Table 1: Solution of velocity profiles and their residuals for $A = 0.07$, $\beta = 0.09$, $d = 0.4$, $\alpha = 0.3$, $\delta = 0.02$, $\varepsilon = 0.001$, $\beta_0 = 0.5$, using OHAM and NIM

y	OHAM Z_0	Residual Z_0	NIM Z_N	Residual Z_N
−1.	2.138×10^{-21}	2.15915×10^{-14}	9.9178×10^{-7}	-5.41652×10^{-13}
−0.9	−0.00232128	9.17904×10^{-15}	−0.0023213	-3.63056×10^{-13}
−0.8	−0.00457666	3.82369×10^{-15}	−0.0045775	-2.31219×10^{-13}
−0.7	−0.00670666	2.06308×10^{-15}	−0.0067083	-1.3803×10^{-13}
−0.6	−0.00865879	1.64202×10^{-15}	−0.0086612	-7.57275×10^{-14}
−0.5	−0.0103876	1.30109×10^{-15}	−0.0103906	-3.70384×10^{-14}
−0.4	−0.0118545	5.4285×10^{-16}	−0.011858	-1.53502×10^{-14}
−0.3	−0.0130281	-6.113×10^{-16}	−0.0130319	-4.90202×10^{-15}
-0.2	−0.0138839	-1.85551×10^{-15}	−0.013888	-9.74738×10^{-16}
−0.1	−0.0144044	-2.80648×10^{-15}	−0.0144086	-6.11524×10^{-17}
0.	−0.014579	-3.16539×10^{-15}	−0.0145833	6.77626×10^{-21}
0.1	−0.0144044	-2.82094×10^{-15}	−0.0144086	-6.11321×10^{-17}
0.2	−0.0138839	-1.88459×10^{-15}	−0.013888	-9.74024×10^{-16}
0.3	−0.0130281	-6.54909×10^{-16}	−0.0130319	-4.89667×10^{-15}
0.4	−0.0118545	4.85848×10^{-16}	−0.011858	-1.53278×10^{-14}
0.5	−0.0103876	1.23373×10^{-15}	−0.0103906	-3.69707×10^{-14}
0.6	−0.00865879	1.56988×10^{-15}	−0.0086612	-7.55606×10^{-14}
0.7	−0.00670666	1.99435×10^{-15}	−0.0067083	-1.37673×10^{-13}
0.8	−0.00457666	3.76807×10^{-15}	−0.0045775	-2.30533×10^{-13}
0.9	−0.00232128	9.14513×10^{-15}	−0.0023213	-3.61837×10^{-13}
1	1.45027×10^{-21}	2.15822×10^{-14}	9.9117×10^{-7}	-5.39622×10^{-13}

$$\begin{aligned}\mathscr{H}_0 = {} & \frac{1+y}{2} + 0.0015309621791103271(1.1151940864635443 - 2.410197299449747 \times 10^{-7}y \\ & - 1.5203012137320218y^2 + 0.5063622206615356y^4 + 3.378447141626716 \\ & \times 10^{-7}y^5 - 0.1012454540934757y^6 - 1.072522902103719 \\ & \times 10^{-7}y^7 - 0.000009639295826571 8y^8 + 1.042730599267505 \times 10^{-8}y^9) \\ & + 9.641485783077917 \times 10^{-12}(5108868.375304848 + 46.84671503095879y \\ & - 6958853.784630358y^2 - 92.4744042260749y^3 + 2307374.36695446y^4 \\ & + 63.95382500511337y^5 - 455119.2829548307y^6 - 20.298040361950047y^7 \\ & - 2269.5077946078723y^8 + 1.971624674137855y^9 - 0.16975627150116573y^{10} \\ & + 0.0002798755802494539y^{11} + 0.003079742117630905y^{12} + 2.515856851532262 \\ & \times 10^{-9}y^{13} - 0.00020294369111940546y^{14} - 2.951747499482099 \times 10^{-10}y^{15} \\ & - 1.466066957061849 \times 10^{-8}y^{16} + 1.399338501108967 \times 10^{-11}y^{17}) \end{aligned} \quad . \tag{39}$$

The solutions of velocity Z_N and temperature $\mathscr{H}_N$ up to second order using NIM are

Table 2: Solution of temperature distributions and their residuals for $A = 0.07$, $\beta = 0.09$, $d = 0.4$, $\alpha = 0.3$, $\delta = 0.02$, $\varepsilon = 0.001$, $\beta_0 = 0.5$, using OHAM and NIM

y	OHAM $\mathscr{H}_0$	Residual $\mathscr{H}_0$	NIM $\mathscr{H}_N$	Residual $\mathscr{H}_N$
−1.	−0.0011093	5.12015×10^{-14}	−0.0011093	5.12015×10^{-14}
−0.9	0.049052	1.60448×10^{-11}	0.049052	1.60448×10^{-11}
−0.8	0.099212	1.92037×10^{-11}	0.099212	1.92037×10^{-11}
−0.7	0.149368	1.61215×10^{-11}	0.149368	1.61215×10^{-11}
−0.6	0.199516	1.10242×10^{-11}	0.199516	1.10242×10^{-11}
−0.5	0.249652	6.28037×10^{-12}	0.249652	6.28037×10^{-12}
−0.4	0.299771	2.90004×10^{-12}	0.299771	2.90004×10^{-12}
−0.3	0.349868	9.99103×10^{-13}	0.349868	9.99103×10^{-13}
−0.2	0.39994	2.08946×10^{-13}	0.39994	2.08946×10^{-13}
−0.1	0.449985	1.34953×10^{-14}	0.449985	1.34953×10^{-14}
0.	0.5	0.	0.5	0.
0.1	0.549985	1.3492×10^{-14}	0.549985	1.3492×10^{-14}
0.2	0.59994	2.08866×10^{-13}	0.59994	2.08866×10^{-13}
0.3	0.649868	9.98539×10^{-13}	0.649868	9.98539×10^{-13}
0.4	0.699771	2.89786×10^{-12}	0.699771	2.89786×10^{-12}
0.5	0.749652	6.27446×10^{-12}	0.749652	6.27446×10^{-12}
0.6	0.799516	1.10117×10^{-11}	0.799516	1.10117×10^{-11}
0.7	0.849368	1.61003×10^{-11}	0.849368	1.61003×10^{-11}
0.8	0.899212	1.91749×10^{-11}	0.899212	1.91749×10^{-11}
0.9	0.949052	1.60177×10^{-11}	0.949052	1.60177×10^{-11}
1.	0.998891	5.10503×10^{-14}	0.998891	5.10503×10^{-14}

Table 3: Comparison of velocity and temperature for $A = 2,\ \beta = 0.4, d = 0.02,\ \alpha = 0.3, \delta = 0.01,\ \varepsilon = 0.4,\ \beta_0 = 0.9$, using OHAM and NIM

y	NIM Z_N	OHAM Z_0	Difference	NIM $\mathscr{H}_N$	OHAM $\mathscr{H}_0$	Difference
−1	0.000558612	-9.592×10^{-19}	5.58×10^{-4}	−0.0230161	1.2873×10^{-18}	0.0230161
−0.8182	−0.119032	−0.118607	4.25×10^{-4}	0.0739715	0.0968961	0.022925
−0.6162	−0.238746	−0.237459	1.28×10^{-3}	0.181403	0.204237	0.022834
−0.4141	−0.33336	−0.331455	1.91×10^{-3}	0.287883	0.310644	0.022761
−o.2121	−0.394341	−0.39206	2.28×10^{-3}	0.392565	0.415279	0.022714
−0.0101	−0.416616	−0.414202	2.42×10^{-3}	0.494947	0.517644	0.022697
0.0101	−0.416616	−0.414202	2.42×10^{-3}	0.505047	0.527744	0.022697
0.2121	−0.394341	−0.392061	2.28×10^{-3}	0.604665	0.627379	0.022714
0.4141	−0.33336	−0.331456	1.91×10^{-3}	0.701983	0.724744	0.022761
0.6162	−0.238746	−0.23746	1.28×10^{-3}	0.797603	0.820437	0.022834
0.8182	−0.119033	−0.118607	4.26×10^{-4}	0.892172	0.915096	0.022924
1	0.000556465	-1.034×10^{-18}		0.976984	1.	0.023016

Table 4: Comparison of velocity and temperature for $A = 2,\ \beta = 0.4, d = 0.03,\ \alpha = 0.3, \delta = 0.21,\ \varepsilon = 0.4,\ \beta_0 = 0.7$, using OHAM and NIM

y	NIM Z_N	OHAM Z_0	Difference	NIM $\mathscr{H}_N$	OHAM $\mathscr{H}_0$	Difference
−1	0.000556221	-7.33041×10^{-19}	5.56×10^{-4}	−0.0460314	8.02454×10^{-18}	0.0460314
−0.9192	−0.0532931	−0.0533902	9.71×10^{-5}	−0.00019996	0.0457495	0.045949
−0.7172	−0.181375	−0.180495	8.80×10^{-4}	0.114132	0.159887	0.045755
−0.5152	−0.289781	−0.288166	1.62×10^{-3}	0.227181	0.272771	0.04559
−0.3131	−0.368446	−0.366338	2.11×10^{-3}	0.337517	0.382987	0.04547
−0.1111	−0.410508	−0.408148	2.36×10^{-3}	0.443682	0.489088	0.045406
0.1111	−0.410508	−0.408149	2.36×10^{-3}	0.554782	0.600188	0.045406
0.3131	−0.368446	−0.366341	2.11×10^{-3}	0.650617	0.696087	0.04547
0.5152	−0.289781	−0.28817	1.61×10^{-3}	0.742382	0.787971	0.045589
0.7172	−0.181376	−0.180498	8.78×10^{-4}	0.831333	0.877086	0.045753
0.9192	−0.0532966	−0.0533911	9.45×10^{-5}	0.919002	0.964949	0.045947
1	0.000550897	-9.13904×10^{-19}	5.51×10^{-5}	0.953971	1.	0.046029

Table 5: Comparison of velocity and temperature for $A = 1,\ \beta = 0.3, d = 0.04,\ \alpha = 0.8,\ \delta = 0.07,\ \varepsilon = 0.3,\ \beta_0 = 0.6$, using NIM and OHAM

y	NIM Z_N	OHAM Z_0	Difference	NIM $\mathscr{H}_N$	OHAM $\mathscr{H}_0$	Difference
−1	0.00111137	-7.34818×10^{-19}	1.1×10^{-3}	−0.0725337	-5.14×10^{-19}	0.0725337
−0.8586	−0.0460644	−0.0456431	4.21×10^{-4}	0.0132899	0.0849699	0.07168
−0.6566	−0.108083	−0.105884	2.19×10^{-3}	0.134998	0.205563	0.070565
−0.4545	−0.158419	−0.154922	3.49×10^{-3}	0.25392	0.323587	0.069667
−0.2525	−0.192559	−0.188239	4.32×10^{-3}	0.367674	0.436736	0.069062
−0.0505	−0.207696	−0.203026	4.67×10^{-3}	0.474502	0.543297	0.068795
0.0505	−0.207696	−0.203028	4.67×10^{-3}	0.525002	0.593797	0.068795
0.2525	−0.192559	−0.188246	4.31×10^{-3}	0.620174	0.689236	0.069062
0.4545	−0.158419	−0.15493	3.48×10^{-3}	0.70842	0.778086	0.069666
0.6566	−0.108085	−0.105892	2.19×10^{-3}	0.791601	0.862161	0.07056
0.8586	−0.0460714	−0.0456471	4.24×10^{-4}	0.8719	0.943567	0.071667
1	0.00109683	-1.23234×10^{-18}	1.09×10^{-3}	0.927486	1.	0.072514

Table 6: Comparison of velocity and temperature for $A = 1.5,\ \beta = 0.2, d = 0.05,\ \alpha = 0.1, \delta = 0.02,\ \varepsilon = 0.2, \beta_0 = 0.5$, using NIM and OHAM

y	NIM (Z_N)	OHAM (Z_0)	Difference	NIM $\mathscr{H}_N$	OHAM $\mathscr{H}_0$	Difference
−1	0.0000115351	-4.7676×10^{-21}	1.15×10^{-5}	−0.103137	-1.42074×10^{-16}	0.103137
−−0.9596	−0.0201738	−0.0201805	6.7×10^{-6}	−0.0768761	0.0762387	0.153115
−0.7576	−0.117851	−0.117837	1.4×10^{-5}	0.0541516	0.450492	0.39634
−0.5556	−0.202695	−0.202664	3.1×10^{-5}	0.18298	0.79912	0.61614
−0.3535	−0.266615	−0.266573	4.2×10^{-5}	0.306391	1.09603	0.789639
−0.1515	−0.303926	−0.303877	4.9×10^{-5}	0.421047	1.31553	0.894483
0.1515	−0.303926	−0.303878	4.8×10^{-5}	0.572547	1.46706	0.894513
0.3535	−0.266615	−0.266573	4.2×10^{-5}	0.659891	1.44956	0.789669
0.5556	−0.202695	−0.202664	3.1×10^{-5}	0.73858	1.35467	0.61609
0.7576	−0.117851	−0.117837	1.4×10^{-5}	0.811752	1.20797	0.396218
0.9596	−0.020174	−0.0201805	6.5×10^{-6}	0.882724	1.03579	0.153066
1	0.0000113541	-3.62385×10^{-21}	1.13×10^{-5}	0.896863	1.	0.103137

$$
\begin{aligned}
Z_N = {} & (1/24)(-0.4 + 0.48y^2 - 0.08y^4) + 0.010000000000000002(-2.571062875487445 \\
& \times 10^{-17}y^5(4.915200000000004 \times 10^{-16}y^5)(-367567200 - 292383000y + 19492200y^2 \\
& + 72870840y^3 + 9951120y^4 - 7095528y^5 - 1624095y^6 + 238095y^7 + 70070y^8) \\
& + 3172.6079999999997(0.419328y(-6930 + 1485y^2 - 209y^4 + 14y^6) \\
& + 0.00001600000000000001y^2(2162160 - 60060y^2 - 1.8450432000000003y^3 \\
& + 0.3913728y^5 - 0.03391488000000001y^7 + 0.00101376y^9) \\
& + 0.06000000000000001(15135120 - 720720y^2 - 8.302694400000002y^3 \\
& + 2.0602982400000003y^5 - 0.24600576000000005y^7(+0.010014720000000003y^9)) \\
& - 0.000010368000000000005y^2(0.052224y(-4054050 - 1501500y) + 1006005y^2 \\
& + 449085y^3 - 120120y^4 - 59535y^5 + 4890y^6 + 2849y^7) \\
& + 0.010000000000000002(1470268800 + 367567200y - 40840800y^2 - 1.6338829258752 \\
& \times 10^7y^3 - 998.0006400000002y^4 + 532.267008y^5 + 248.73246720000003y^6 \\
& - 46.124236800000006y^7 - 24.219402240000004y^8((+1.3787136000000002y^9 \\
& + 0.8126976000000001y^{10}))) - 8.57020958495815 \\
& \times 10^{-15}y^4(3.7042305011712 \times 10^7(-840 + 55.9552y^2) + 0.0016000000000000007y^4) \\
& + 4.915200000000005 \times 10^{-19}y^6(-827026200 - 666633240y + 11695320y^2 + 146127240y^3 \\
& + 24069960y^4 - 12938904y^5 - 3222945y^6 + 456885y^7 + 140140y^8) \\
& + 1.1897280000000001(3.354624y^2(-3465 + 990y^2 - 99y^4 + 7y^6) \\
& + 0.00001600000000000001y^2(242161920 + 86486400y - 8648640y^2 - 4324320y^3 \\
& - 11.0702592y^4 + 2.0351385600000005y^6 - 0.15851520000000002y^8 \\
& + 0.005068800000000001y^{10}) + 0.24000000000000005(151351200 + 30270240y \\
& - 10090080y^2 - 4324320y^3 - 11.0702592y^4 \\
& + 2.5523097600000004y^6(-0.25718784000000006y^8 + 0.011059200000000002y^{10})) \\
& - 1.0368 \times 10^{-8}y^2(0.026112y^2(-16216200 - 5855850y + 3738735y^2) + 1597050y^3 \\
& - 376740y^4 - 188790y^5 + 16200y^6 + 9394y^7) + 0.010000000000000002(30875644800 \\
& + 22054032000y + 3308104800y^2 - 1102701600y^3 - 2.94059405832192 \times 10^8y^4 \\
& - 2275.4414592000003y^5 + 1037.9206656000001y^6 + 498.78097920000005y^7 \\
& - 80.84275200000002y^8(((-44.164792320000004y^9 + 2.5850880000000007y^{10} \\
& + 1.5595008000000001y^{11}))),
\end{aligned}
\tag{40}
$$

$$\begin{aligned}\mathcal{H}_N = {} & \frac{1+y}{2} - 0.03(-6.481744733654794 \times 10^{-11}(-328672.36491264y^4 + 274.274574336y^5 + 87575.06691128918y^6 \\ & - 86.96695300669442y^7 - 7808.813218777303y^8 + 8.438224438722099y^9 - 0.8941928379923474y^{10} \\ & + 0.001473865673660899y^{11} + 0.01618888476556816y^{12} + 8.807963874134526 \\ & \times 10^{-8}y^{13} - 0.0010668166769821899y^{14} - 3.681492026907573 \times 10^{-9}y^{15} - 2.067067519143527 \times 10^{-7}y^{16} \\ & + 1.793178953955856 \times 10^{-10}y^{17} - 1.37411630808001 \times 10^{-11}y^{18} + 2.412960087947417 \times 10^{-14}y^{19} \\ & - 3.221587165756582 \times 10^{-16}y^{20} + 8.276225275611434 \times 10^{-19}y^{21} \\ & - 7.343436467532474 \times 10^{-22}y^{22} + 2.17589881422925 \times 10^{-25}y^{23}) + 6.185705774183141 \\ & \times 10^{-8}y^2(2.560000000000002 \times 10^{-12}y^4(41{,}580 + 39{,}600y + 2{,}475y^2 - 8{,}470y^3 - 2{,}079y^4 + 504y^5 + 168y^6) \\ & - 0.000002304y^2(207{,}900 + 83{,}160y - 96953.472y^2 - 47488.32000000001y^3 + 7413.12y^4 + 4613.224y^5 \\ & + 0.6160000000000002y^6 + 0.40320000000000017y^7) \\ & + 28.511999999999997(45{,}360 - 15107.904y^2 + 3018.35713536y^4 + 0.43165440000000016y^6 \\ & + 0.00001792000000000015y^8))).\end{aligned} \tag{41}$$

4.1 Volume flux

Volume flux in dimensionless form,

$$Q = \int_{-1}^{1} Z\,dy. \tag{42}$$

Substituting Eqs. (38) and (40) in Eq. (42) implies

$$\begin{aligned}Q_0 = {} & 0. - \frac{4A}{15} + 0.1079A\beta^2\alpha^2 - 0.0437A\beta^4\alpha^4 \\ & - \frac{0.0115A\beta^4d^2\alpha^4\varepsilon^2}{\beta_0^4} + \frac{0.00052A^3\beta^2d^2\alpha^4\varepsilon^2\delta}{\beta_0^4} \\ & - \frac{0.0539A\beta^2d\alpha^2\varepsilon}{\beta_0^2} + \frac{0.04372A\beta^4d\alpha^4\varepsilon}{\beta_0^2} \\ & - \frac{0.0039707A^3d\alpha^2\varepsilon\delta}{\beta_0^2} - \frac{0.00103282A^3\beta^2d\alpha^4\varepsilon\delta}{\beta_0^2}\end{aligned}. \tag{43}$$

$$\begin{aligned}Q_N = {} & -\frac{4A}{15} + \frac{1}{126}A\beta^2\alpha^2 + \frac{A\beta^4\alpha^4}{5{,}184} \\ & + \frac{792{,}750{,}407A^3\beta^4d^3\alpha^6\varepsilon^3\delta}{7{,}602{,}818{,}775{,}552{,}000\beta_0^6} + \frac{1{,}093A\beta^4d^2\alpha^4\varepsilon^2}{19{,}958{,}400\beta_0^4} \\ & - \frac{1{,}232{,}423A^3\beta^2d^2\alpha^4\varepsilon^2\delta}{217{,}945{,}728{,}000\beta_0^4} \\ & - \frac{5{,}474{,}983A^3\beta^4d^2\alpha^6\varepsilon^2\delta}{14{,}820{,}309{,}504{,}000\beta_0^4} - \frac{A\beta^2d\alpha^2\varepsilon}{252\beta_0^2} \\ & - \frac{A\beta^4d\alpha^4\varepsilon}{5{,}184\beta_0^2} + \frac{16073A^3d\alpha^2\varepsilon\delta}{129{,}729{,}600\beta_0^2} \\ & + \frac{1{,}232{,}423A^3\beta^2d\alpha^4\varepsilon\delta}{108{,}972{,}864{,}000\beta_0^2} + \frac{5{,}474{,}983A^3\beta^4d\alpha^6\varepsilon\delta}{14{,}820{,}309{,}504{,}000\beta_0^2}.\end{aligned} \tag{44}$$

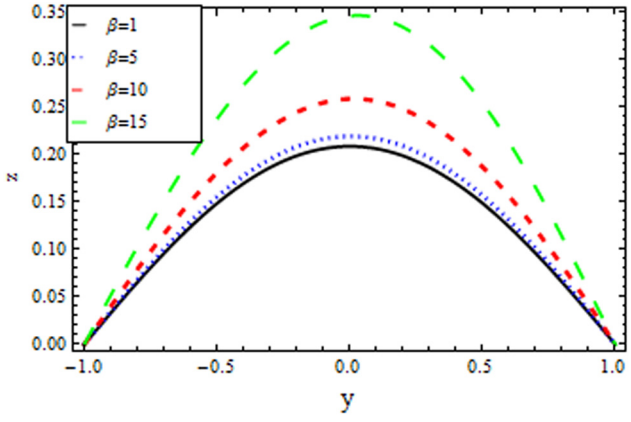

Figure 2: The velocity profile for $\beta_0 = 0.009$, $d = 5$, $A = -1$, $\varepsilon = 0.01$, $\delta = 3$, and $\alpha = 0.004$, employing OHAM.

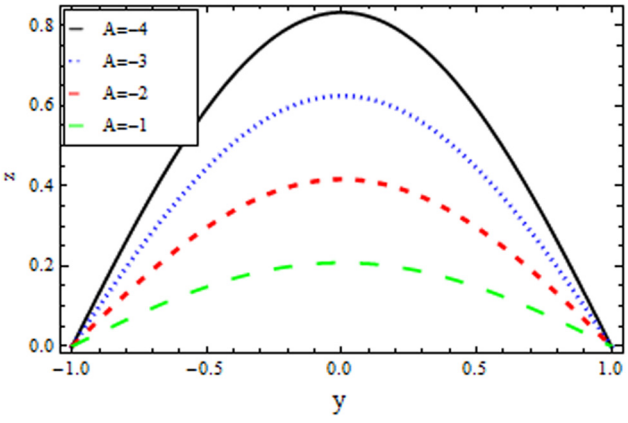

Figure 3: The velocity profile for $d = 2$, $\beta = 0.1$, $\alpha = 0.003$, $\beta_0 = 1$, $\delta = 3$, and $\varepsilon = 0.01$, employing OHAM.

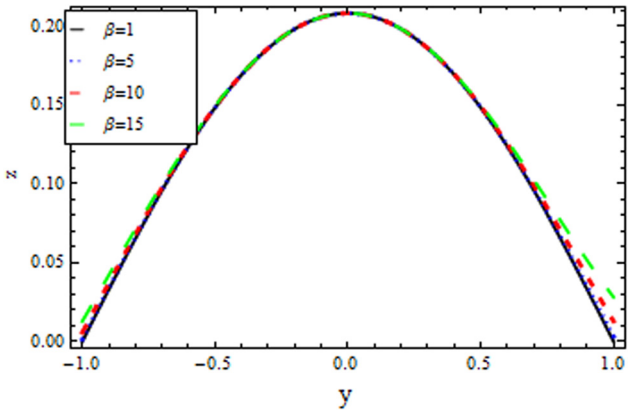

Figure 4: The velocity for $\beta_0 = 0.009$, $d = 5$, $\alpha = 0.004$, $\varepsilon = 0.01$, $\delta = 3$, and $A = -1$, employing NIM.

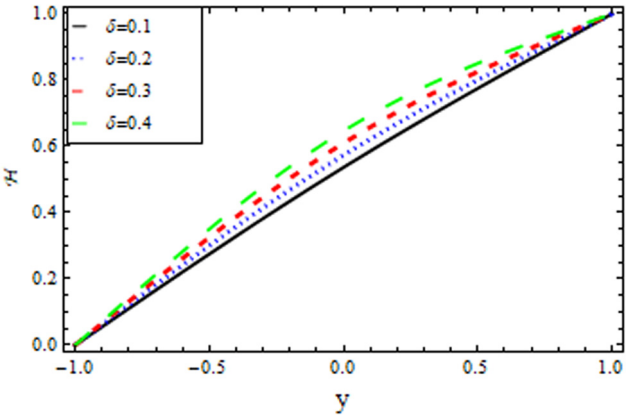

Figure 7: Temperature distribution for $A = 0.2$, $\beta_0 = 0.1$, $\alpha = 0.004$, $\varepsilon = 0.001$, $\beta = 0.1$, and $d = 0.5$, using OHAM.

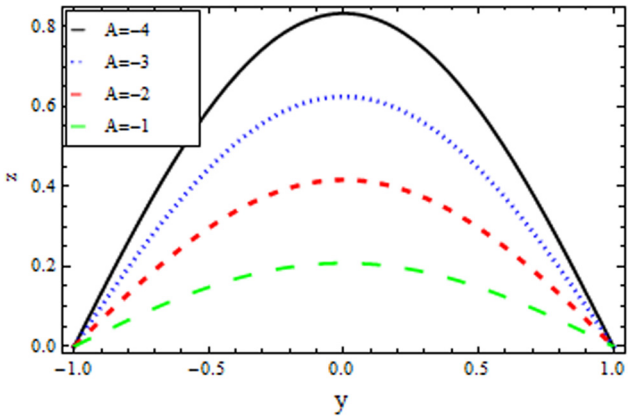

Figure 5: The velocity for $\varepsilon = 0.01$, $\beta_0 = 0.1$, $\alpha = 0.003$, $\beta_0 = 1$, $\delta = 3$, and $d = 2$, employing NIM.

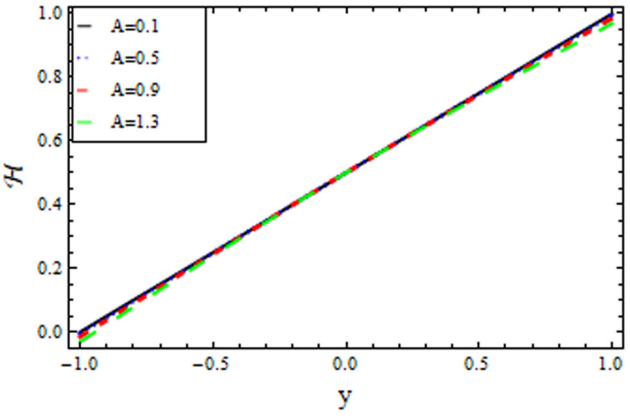

Figure 8: Temperature distribution for $\alpha = 0.003$, $\beta_0 = 1$, $\delta = 0.002$, $\varepsilon = 0.001$, $\beta = 0.1$, and $d = 0.5$, using NIM.

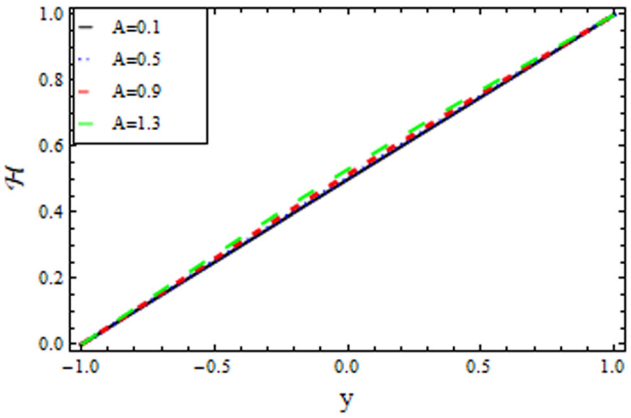

Figure 6: Temperature distribution for $\alpha = 0.003$, $\beta_0 = 1$, $\delta = 0.002$, $\varepsilon = 0.001$, $\beta = 0.1$, and $d = 0.5$, using OHAM.

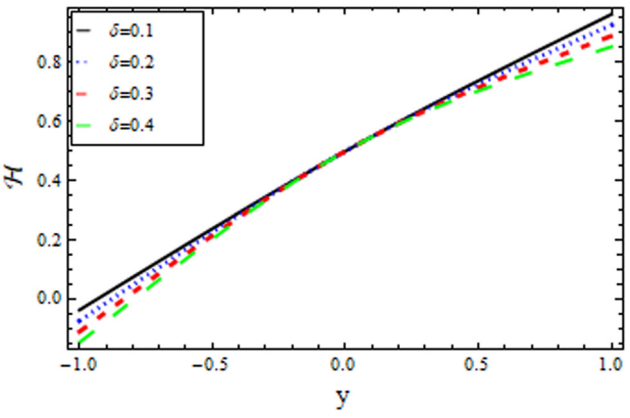

Figure 9: Temperature distributions for $A = 0.2$, $\beta_0 = 0.1$, $\alpha = 0.004$, $\varepsilon = 0.001$, $\beta = 0.1$, and $d = 0.5$, using NIM.

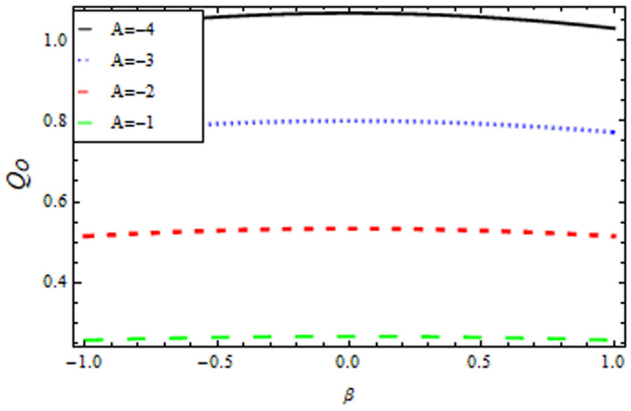

Figure 10: The volume flux for $\varepsilon = 0.001$, $\beta_0 = 1$, $d = 0.4$, $\delta = 4$, and $\alpha = 0.3$, using OHAM.

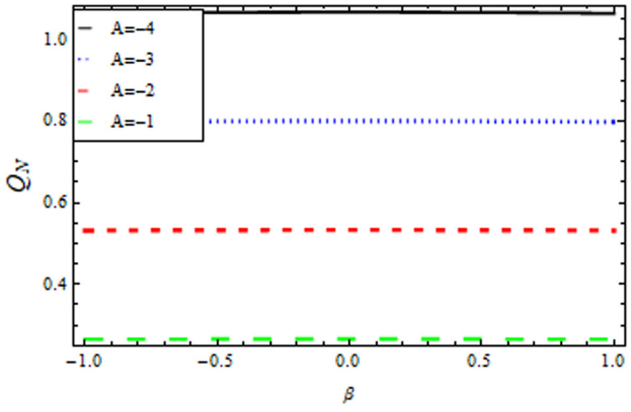

Figure 11: The volume flux for $\varepsilon = 0.001$, $\beta_0 = 1$, $d = 0.4$, $\delta = 4$, and $\alpha = 0.3$, using NIM.

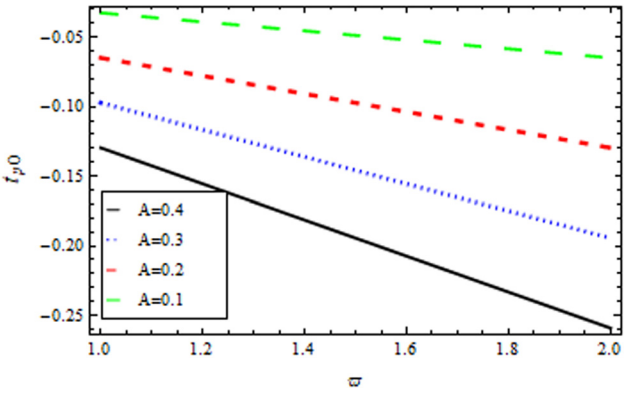

Figure 12: Shear stress for $\delta = 0.02$, $\beta = 0.9$, $d = 0.4$, $\beta_0 = 0.5$, $\alpha = 0.3$, and $\varepsilon = 0.001$, employing OHAM.

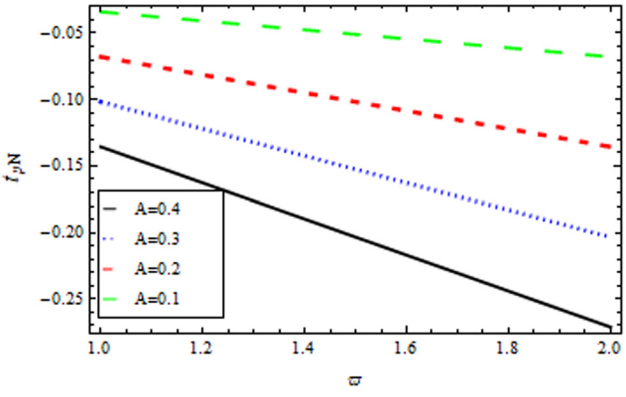

Figure 13: Shear stress for $\delta = 0.02$, $\beta = 0.9$, $\varepsilon = 0.001$, $\beta_0 = 0.5$, $\alpha = 0.3$, and $d = 0.4$, using NIM.

4.2 Average velocity

The average velocity, $\bar{z}$ is as follows:

$$\bar{z} = \frac{Q}{d}. \tag{45}$$

In dimensionless form (45) matched with the flow rate in (43) and (44).

4.3 Shear stress

Shear stress in dimensionless form is

$$t_{\not\prime} = -\varpi D[z, y], \quad y = 1. \tag{46}$$

The negative sign in Eq. (46) is because the upper wall confronts the negative $y-$direction of the coordinate system [34]. Here $t_{\not\prime 0}$, $t_{\not\prime N}$, Q_0, and Q_N are the shear stresses and volume fluxes, obtained employing both methods.

5 Results and discussion

With the parameters A, β_0, β, d, α, δ, and ε, we looked at how the velocity, temperature, average velocity, volume flux, and shear stress varied in this study. Solutions for the velocity profile, temperature distributions, and residual utilizing OHAM and NIM are given in Tables 1 and 2. The absolute differences in the temperature distributions and velocity profiles for various parameters using both approaches are shown in Tables 3–6. The velocity profile of OHAM (Figures 2 and 3) and that of NIM (Figures 4 and 5) are in good agreement. Fluid velocity increases in the middle of the plates in both situations before vanishing on either plate. Using various

parameters, Figures 6 and 7 represent the temperature distributions of OHAM. Figures 8 and 9 show the temperature distributions of NIM. As fluid travels from lower to upper plates, its temperature rises, and in cases, its velocity and temperature is highly dependent on the parameters A, β_0, β, d, α, δ and ε. In the said techniques, temperature increases when the parameter δ increases. The volume flux of the fluid is investigated in Figures 10 and 11 for both techniques. In these figures, we can notice the influence of the parameters. Increasing the value of A reduces the volume flux of the fluid, which is inversely related between A and Q. Figures 12 and 13 show the behavior of shear stress $t_{\not p}$ in the considered fluid flow, when varying the value of the parameter A, for both the techniques. The relationship between A and $t_{\not p}$ can be observed in these figures.

6 Conclusion

In this study, we have studied the flow of couple stress fluids of Vogel's model between two parallel plates, with the help of OHAM and NIM. Employing the said methods, the approximate solutions of the strongly nonlinear differential equations of couple stress fluids of Vogel's model for velocity profile, temperature distributions, average velocity, volume flux, and shear stress on the plates have been obtained. The velocity profile and temperature distributions obtained using these methods are in good agreement, velocity and temperature distributions of both methods are strongly dependent on different parameters as illustrated in the figures. The results attained using these techniques are in the form of infinite power series.

Acknowledgments: The authors extend their appreciation to the Deanship of Scientific Research at King Khalid University for funding this work through large group Research Project under grant number RGP2/461/44.

Funding information: This research was funded through large group Research Project under Grant number RGP2/461/44 by the Deanship of Scientific Research at King Khalid University.

Author contributions: All authors have accepted responsibility for the entire content of this manuscript and approved its submission.

Conflict of interest: The authors state no conflict of interest.

References

[1] Harris J. Rheology and non-Newtonian flow. New York: Longman; 1977.
[2] Tan W, Masuoka T. Stokes' first problem for a second grade fluid in a porous half-space with heated boundary. Int J Non-Linear Mech. 2005;40:515–22.
[3] Stokes VK. Theories of fluids with microstructure: An introduction. Berlin-Heidelberg-New York-Tokyo: Springer-Verlag; 1984.
[4] Devakar M, Iyengar TKV. Run up flow of a couple stress fluid between parallel plates. Nonlinear Anal: Model Control. 2010;15:29–37.
[5] Siddiqui AM, Ahmed M, Islam S, Ghori QK. Homotopy analysis of Couette and Poiseuille flows for fourth grade fluids. Acta Mech. 2005;180:117–32.
[6] Hayat T, Ellahi R, Mahomed FM. Exact solutions for Couette and Poiseuille flows for fourth grade fluids. Acta Mech. 2007;188:69–78.
[7] Naduvinamani NB, Fathima ST, Hiremath PS. Effect of surface roughness on characteristics of couple stress squeeze film between anisotropic porous rectangular plates. Fluid Dyn Res. 2003;32:217.
[8] Naduvinamani NB, Fathima ST, Hiremath PS. Hydrodynamic lubrication of rough slider bearings with couple stress fluids. Tribol Int. 2003;36:949–59.
[9] Naduvinamani NB, Hiremath PS, Gurubasavaraj G. Effect of surface roughness on the couple-stress squeeze film between a sphere and a flat plate. Tribol Int. 2005;38:451–8.
[10] Hussain A, Arshad M, Rehman A, Hassan A, Elagan SK, Ahmad H, et al. Three-dimensional water-based magneto-hydrodynamic rotating nanofluid flow over a linear extending sheet and heat transport analysis: A numerical approach. Energies. 2021;14:5133.
[11] Abouelregal AE, Ahmad H, Yao SW. Functionally graded piezoelectric medium exposed to a movable heat flow based on a heat equation with a memory-dependent derivative. Materials. 2020;13:3953.
[12] Jain R, Mehta R, Bhatnagar A, Ahmad H, Khan ZA, Ismail GM. Numerical study of heat and mass transfer of Williamson hybrid nanofluid (CuO/CNT's-water) past a permeable stretching/shrinking surface with mixed convective boundary condition. Case Stud Therm Eng. 2024;59:104313.
[13] Gangadhar K, Sree TS, Thirupathi T. Impact of Arrhenius energy and irregular heat absorption on generalized second grade fluid MHD flow over nonlinear elongating surface with thermal radiation and Cattaneo-Christov heat flux theory. Mod Phys Lett B. 2024;38:2450077.
[14] Ahmad H, Sakhri N, Menni Y, Omri M, Ameur H. Experimental study of the efficiency of earth-to-air heat exchangers: Effect of the presence of external fans. Case Stud Therm Eng. 2021;28:101461.
[15] Djeffal F, Bordja L, Rebhi R, Inc M, Ahmad H, Tahrour F, et al. Numerical investigation of thermal-flow characteristics in heat exchanger with various tube shapes. Appl Sci. 2021;11:9477.
[16] Chinyoka T, Makinde OD. Computational dynamics of unsteady flow of a variable viscosity reactive fluid in a porous pipe. Mech Res Commun. 2010;37:347–53.
[17] Makinde OD. Thermal criticality in viscous reactive flows through channels with a sliding wall: An exploitation of the Hermite-Padé approximation method. Math Compu Model. 2008;47:312–7.

[18] Herisanu N, Marinca V, Dordea T, Madescu G. A new analytical approach to nonlinear vibration of an electrical machine. Proc Rom Acad Ser A-Math Phys Tech Sci Inf Sci. 2008;9:229–36.
[19] Marinca V, Herisanu N. Determination of periodic solutions for the motion of a particle on a rotating parabola by means of the optimal homotopy asymptotic method. J Sound Vib. 2010;329:1450–9.
[20] Nawaz R, Islam S, Shah IA, Idrees M, Ullah H. Optimal homotopy asymptotic method to nonlinear damped generalized regularized long-wave equation. Math Probl Eng. 2013;2013:503137.
[21] Ullah H, Islam S, Idrees M, Nawaz R. Application of optimal homotopy asymptotic method to doubly wave solutions of the coupled Drinfeld-Sokolov-Wilson equations. Math Probl Eng. 2013;2013:362816.
[22] Sheikholeslami M, Hatami M, Ganji DD. Micropolar fluid flow and heat transfer in a permeable channel using analytical method. J Mol Liq. 2014;194:30–6.
[23] Anjum A, Mir NA, Farooq M, Javed M, Ahmad S, Malik MY, et al. Physical aspects of heat generation/absorption in the second grade fluid flow due to Riga plate: Application of Cattaneo-Christov approach. Results Phys. 2018;9:955–60.
[24] Gejji V, Jafari H. An iterative method for solving nonlinear functional equations. J Math Anal Appl. 2006;316:753–63.
[25] Bhalekar S, Gejji V. Solving fractional-order logistic equation using a new iterative method. Int J Differ Equ. 2012;2012:975829.
[26] Bhalekar S, Daftardar-Gejji VD. Convergence of the new iterative method. Int J Differ Equ. 2011;2011:989065.
[27] Siddiqui AM, Ahmed M, Ghori QK. Couette and Poiseuille flows for non-Newtonian fluids. Int J Nonlinear Sci Numer Simul. 2006;7:15–26.
[28] Farooq M, Khan A, Nawaz R, Islam S, Ayaz M, Chu YM. Comparative study of generalized couette flow of couple stress fluid using optimal homotopy asymptotic method and new iterative method. Sci Rep. 2021;11:3478.
[29] Khan A, Farooq M, Nawaz R, Ayaz M, Islam S. Comparative study of plane Poiseuille flow of non-isothermal couple stress fluid of Reynold viscosity model using optimal homotopy asymptotic method and new iterative method. J Appl Comput Mech. 2021;7:404–14.
[30] Islam S, Ali I, Ran XJ, Shah A, Siddiqui AM. Effects of couple stresses on Couette and Poiseuille flow. Int J Non-linear Sci Numer Simmulations. 2009;10:99–112.
[31] Massoudi M, Christie I. Effects of variable viscosity and viscous dissipation on the flow of a third grade fluid in a pipe. Int J Non-Linear Mech. 1995;30:687–99.
[32] Makinde OD. Hermite-Padé approximation approach to thermal criticality for a reactive third-grade liquid in a channel with isothermal walls. Int Commun Heat Mass Transf. 2007;34:870–7.
[33] Marinca V, Herişanu N, Nemeş I. Optimal homotopy asymptotic method with application to thin film flow. Open Phys. 2008;6:648–53.
[34] Papanastasiou T, Georgiou G, Alexandrou AN. Viscous fluid flow. New York: CRC Press; 1999.